Applied Thermal Engineering 31 (2011) 3428–3436

Contents lists available at ScienceDirect

Applied Thermal Engineering

journal homepage: www.elsevier.com/locate/apthermeng

Hyperbolic boiler tube leak location based on quaternary acoustic array

Liansuo An [a], Peng Wang [a,*], Augusto Sarti [b], Fabio Antonacci [b], Jie Shi [a]

[a] Key Laboratory of Condition Monitoring and Control for Power Plant Equipment Ministry of Education, North China Electric Power University, No.2 BeiNong Road, HuiLongGuan, ChangPing, 102206 Beijing, China
[b] Image and Sound Processing Group, Department of Electronics and Information, Politecnico di Milan, 20133 Milan, Italy

ARTICLE INFO

Article history:
Received 20 April 2011
Accepted 21 June 2011
Available online 30 June 2011

Keywords:
Boiler leakage
Hyperbolic location
Quaternary acoustic array
Time differences of arrival (TDOA)
Maximum likelihood (ML) estimator
Genetic algorithm (GA)

ABSTRACT

Early detection and location of a boiler leak help reduce possible equipment damage and productivity loss. In the present study, a four-element acoustic array and a set of hyperbolic equations were used to locate a power plant boiler leak.

Maximum likelihood (ML) and phase transformation (PHAT) estimators were used to localize the leak source. Error rate and root mean square error (RMSE) evaluation revealed the superiority of ML over PHAT in the noisy and lowly reverberant boiler environment.

To avoid distant source assumption, a genetic algorithm (GA) modified by an adaptive Gaussian mutation operator was used to search for the global hyperbolic optimum by probability calculations. The GA slightly outperformed the quasi-Newton method and required more time to converge. However, selecting a starting point near the true position is not simple in practice, and iterative process convergence is not assured in the quasi-Newton method.

Time delay estimator errors greatly influence localization accuracy. The quaternary plane array localization error was within the permitted range of 0.01 ms, whereas that of the stereo array was 0.1 ms. Compared with the quaternary plane, the stereo array was more robust and accurate, but required more time to converge.

© 2011 Elsevier Ltd. All rights reserved.

1. Introduction

Utility and industrial power plants are very important in today's electricity-dependent world. Boiler Tube Failures (BTF), which causes approximately 60% of boiler outages, may be prevented by early boiler tube leak detection during operation. Early detection helps reduce secondary damage to pressure parts and the resulting productivity loss caused by unscheduled boiler shutdowns. More importantly, the safety of operators is ensured.

Acoustic leak detection is predominantly used in large commercial boilers due to its many advantages, such as real-time detection, remote monitoring capability, and high sensitivity [1,2]. The main technique in acoustic leak detection involves positioning microphones at specific boiler areas to detect sound pressure amplitude. The amplitude obtained from each microphone is then compared with frequency domain data. These acoustic data can further be refined for comparing with historical threshold data to determine the probability of a leak. For instance, if a microphone signals an alarm, the leakage source can be deduced within 10 m-radius hemisphere. Therefore, the acoustic technique plays a major role in identifying the heating surface, which is impossible to locate in a specific tube-row [3–5]. A manpower search of a boiler aperture even as small as 1–4 mm is very time consuming. Accurate leak location is also a crucial issue in a manual search [6].

In the present study, we focused on the relationships among the microphone sensor data using the time differences of arrival (TDOA) strategy. A model of hyperbolic leak location is first established in Section 2. In Section 3, the TDOA of the passive signals received by the specifically positioned sensors are measured using the maximum likelihood (ML) estimator. A genetic algorithm (GA) modified by an adaptive Gaussian mutation operator is used to search for the globally optimum parameters. In Section 4, highly nonlinear hyperbolic equations are constructed from the TDOA measurements. Section 5 discusses the effects of time delay estimator errors on localization accuracy. Conclusions are drawn in Section 6.

2. Model of leakage localization using a four-element array

A leakage localization method, which designs the acoustic array for the TDOA source location, is critical. Linear sensor arrays can locate a leak position only in two dimensions [7]. Plane and stereo

* Corresponding author. Tel.: +39 3891034708.
E-mail address: wangpeng56401126@gmail.com (P. Wang).

1359-4311/$ – see front matter © 2011 Elsevier Ltd. All rights reserved.
doi:10.1016/j.applthermaleng.2011.06.028

Nomenclature

τ_{ij}	time difference of arrival
φ	sound pressure attenuation coefficient
N_p	population size
p_r	probabilities of reproduction
P_c	probability of crossover
P_m	probability of mutation
$\hat{R}_{ss}(n)$	cross-correlation function
$h_i(n)$	acoustical transfer function
$W(\omega)$	frequency weighting function
$\hat{G}_{ss}(\omega)$	power spectrum function
$\gamma(\omega)$	modular square coherence function
SNR	signal to noise ratio, dB
RT	reverberation time, s
RMSE	root mean square error

Subscripts

M	microphone
s	source
p	population
r	reproduction
c	crossover
m	mutation

arrays can accurately pinpoint leak positions, but the stereo algorithm is more complex [8]. A cross array can more accurately locate a leak using five or more elements depending on the number of sensors, but with increased computational costs. Circle [9], sphere, and cylinder arrays show favorable measurement performances, but their structures restrict them to furnace chamber applications.

Four-element plane and stereo arrays were adopted in the present study to localize leakage. The distribution of sensors is schematically illustrated in Fig. 1. The distribution can be modified accordingly depending on the boiler situation.

The four-element microphone array geometry used for fixing the leakage position is shown in Fig. 2 (Suppose Mic. 1 to be the reference microphone.). The leakage source S is assumed to be at an unknown position (x, y, z), whereas the sensors M_1, M_2, M_3 and M_4 are at known locations. τ_{ij} stands for the TDOA between the signal radiations from the source to M_i and M_j.

The leakage source is associated with the following hyperbolic location equation:

$$\|M_i - S\| - \|M_j - S\| = c\tau_{ij} \tag{1}$$

We applied the four-element array in a 1025 t/h circulating fluidized bed boiler in a domestic power plant. The boiler has the following features: $a = 12$ m and $b = 14.6$ m. To provide an explicit solution to the hyperbolic curves defined by the TDOA, far-field $r \gg a, b$, r represents the range between source and array center, was assumed and was subsequently utilized for linearization [10,11]. Carter [12] derived an exact formula for sonar and radar source range and bearing. Although the formula is valid for distant sources, the condition $r \gg a, b$ is not satisfied in the boiler, as illustrated by the SG-1025/17.5-M723 typical boiler (depth = 13.64 m, width = 14.022 m, sensor detection range = ~20 m). Therefore, far-field assumption can have a significant influence on the position fixing. In the field of cellular mobile communications, the Taylor series method [13] starts with an initial estimate, which is improved at each step by determining the local linear least-squares solution. An initial estimate is close to the local minima. Chan [14] proposed a two-step weighted least-squares algorithm, wherein the first step solves the linear equations, and the second utilizes the known relationship between the introduced variable and the position. However, this algorithm is restricted to the two-dimensional plane only. The Newton method, which requires the specification of the Hessian matrix of second derivatives for function optimization, is more commonly used in similar studies. The convergence and performance characteristics of the Newton method can be highly sensitive to the initial estimate of the solution provided for the method.

3. Approximation of the ML estimator

To localize the source, the TDOA of the signal received by the two sensors is firstly estimated. Background noise types in the boiler furnace during operation include combustion, burner jet, cross-flow tube rows, and soot blower noises, as well as other mechanical noises. The frequencies mainly centralize within the 250–1000 Hz band. The sound pressure level (SPL) roughly ranges from 110 to 120 dB [15]. Furthermore, given that the furnace is an enclosed space, sound waves from the pressurized tubes are continuously reflected and absorbed by the wall and tube rows surface simultaneously the sound waves then attenuate gradually. Therefore, the signal received by the sensors is a reverberant signal. Considering the existence of both reverberant and noise inferences in the boiler furnace, the leak signals received by the two microphones are:

$$\begin{aligned} x_i(n) &= \varphi_i s(n-\tau) + h_i(n)^* s(n) + n_i(n) \\ x_j(n) &= \varphi_j s(n) + h_j(n)^* s(n) + n_j(n) \end{aligned} \tag{2}$$

where τ is the TDOA, φ_i and φ_j are signal attenuation, $n_i(n)$ and $n_j(n)$ are the additive noises, and $h_i(n)^*s(n)$ and $h_j(n)^*s(n)$ are the reverberations. If the cross-correlation $\hat{R}_{ss}(n)$ or its Fourier transform equivalent $\hat{G}_{ss}(\omega)$ (according to the Wiener–Khinchin theorem) can be recovered, τ can then be estimated as follows:

$$\tau = \arg\max_\tau \hat{R}_{s_i s_j}(n) \tag{3}$$

In practice, $\hat{G}_{ss}(\omega)$ is replaced by $\hat{G}_{x_i x_j}(\omega)$. Various frequencies weighing functions are proposed to deal with the approximation:

$$\hat{R}_{s_1 s_2}(\tau) = \frac{1}{2\pi}\int_{-\pi}^{\pi} \hat{G}_{s_1 s_2}(\omega) e^{j\omega\tau} d\omega \approx \frac{1}{2\pi}\int_{-\pi}^{\pi} W(\omega)\hat{G}_{x_1 x_2}(\omega) e^{j\omega\tau} d\omega \tag{4}$$

where $W(\omega)$ is the frequency weighting function. In practice, choosing the right weighting function is greatly significant. A previous research [16] suggests that the normalized generalized cross-correlation (GCC), i.e., the phase transformation (PHAT) weighing function, deals better with reverberation, as shown in the following equation:

$$W_{\mathrm{PHAT}}(\omega) = \frac{1}{\left|\hat{G}_{x_i x_j}(\omega)\right|^2} \tag{5}$$

On the other hand, ML weight function can be defined as:

$$W_{\mathrm{ML}}(\omega) = \frac{|\gamma(\omega)|^2}{\left|\hat{G}_{x_i x_j}(\omega)\right|\left(1 - |\gamma(\omega)|^2\right)} \tag{6}$$

In the above equation, $|\gamma(\omega)|^2$ is the modular square coherence function expressed as:

$$|\gamma(\omega)|^2 = \frac{\left|\hat{G}_{x_i x_j}(\omega)\right|^2}{\hat{G}_{x_i x_i}(\omega)\hat{G}_{x_j x_j}(\omega)} \tag{7}$$

where $\hat{G}_{x_i x_i}(\omega)$, $\hat{G}_{x_j x_j}(\omega)$, and $\hat{G}_{x_i x_j}(\omega)$ represent the noise auto-power spectrum signal i and the cross-power spectrum signal j.

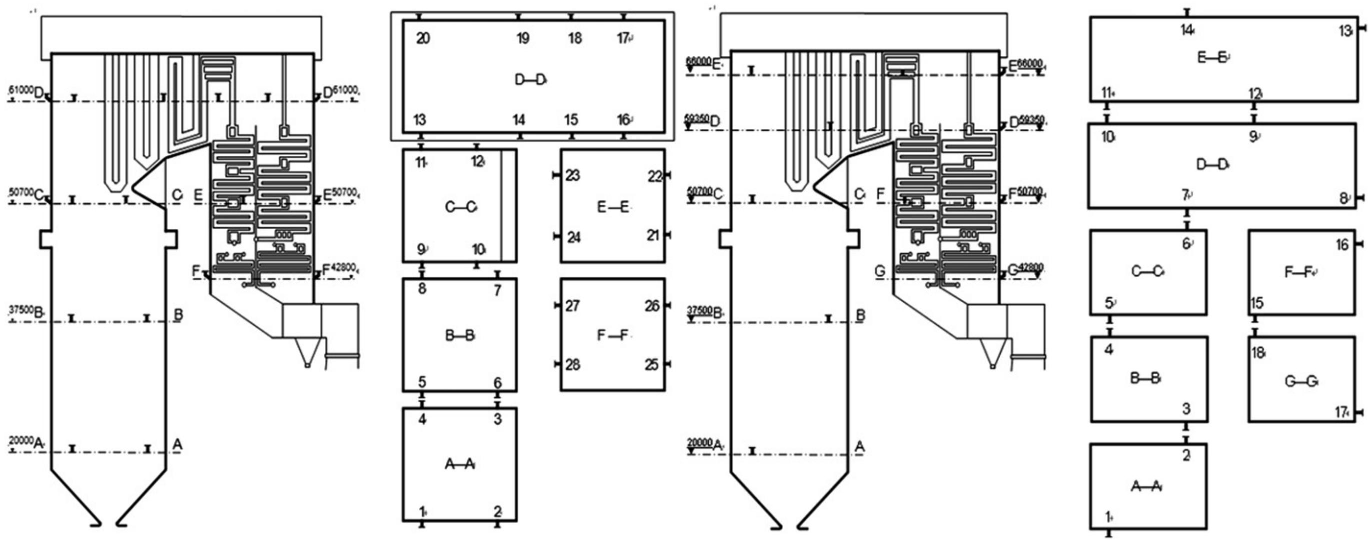

Fig. 1. Distribution of plane and stereo quaternary arrays within the furnace chamber.

We conducted an experiment to evaluate the accuracy of the ML and PHAT estimation methods at various signal-to-noise ratios (SNRs) and low reverberation conditions. The two sensors are M_{11} (7.3, 6, 50.7) as well as M_9 (−7.3, 6, 50.7) in Floor C, and the leak source is at the front wall position (0, 6, 55) (Fig. 1). We simulated the working fluid by air-jet noise instead of water vapor noise. As illustrated in Fig. 3, the leak noise is a continuous broadband signal, and the energy distributes to various frequency components. In conditions of similar outlet pressure and backpressure, the SPL increases with aperture enlargement. A weak frequency peak can be observed between 11 and 16 kHz. The imaging method [17] was used to produce reverberant signals, and the parameters are set to sampling frequency $F_s = 102400$ Hz, sampling frame length = 512, and overlap = 50%.

Fig. 4 shows the normalized frequency (vertical axis), which describes how well the true delay is estimated around the zone of interest. The red dashed line at TDOA = 0 ms is the true delay. The leakage signal is under favorable noise and reverberation conditions in the furnace, where SNR = 10 dB and reverberation time (RT) = 0.2 s. Generally, both ML and PHAT algorithms perform well and have small biases and variances. However, in the present study, when the leakage signal level decreases (SNR = −10 dB), PHAT performance rapidly deteriorates, and anomalies remarkably appear. Therefore, the ML method makes more accurate estimations.

We calculated error percentage and root mean square error (RMSE) in milliseconds. The RMSE of each estimator is considered as more appropriate than the estimator's variance or bias alone. The RMSE is defined by:

$$\mathrm{RMSE}[\hat{\tau}] = \sqrt{\mathrm{bais}\{\hat{\tau}\}^2 + \mathrm{var}\{\hat{\tau}\}} \tag{8}$$

where $\hat{\tau}$ is the estimate of the true value τ. The RMSE value is only obtained from non-anomalous estimates.

After the error rate and RMSE evaluations, the ML estimator was found to possess a distinct performance advantage over PHAT under less favorable noise and low reverberation conditions (Fig. 5).

For practicality, the GCC-based ML estimation was carried out using the LabVIEW software and an NI PXI-6133 data acquisition card under cold boiler conditions. The air-jet noise time domain waveforms are illustrated in Fig. 6. As different leak sound pressure received by four microphones descending: Mic.4 > Mic. 3 > Mic. 1 > Mic.2, caused by the leakage range.

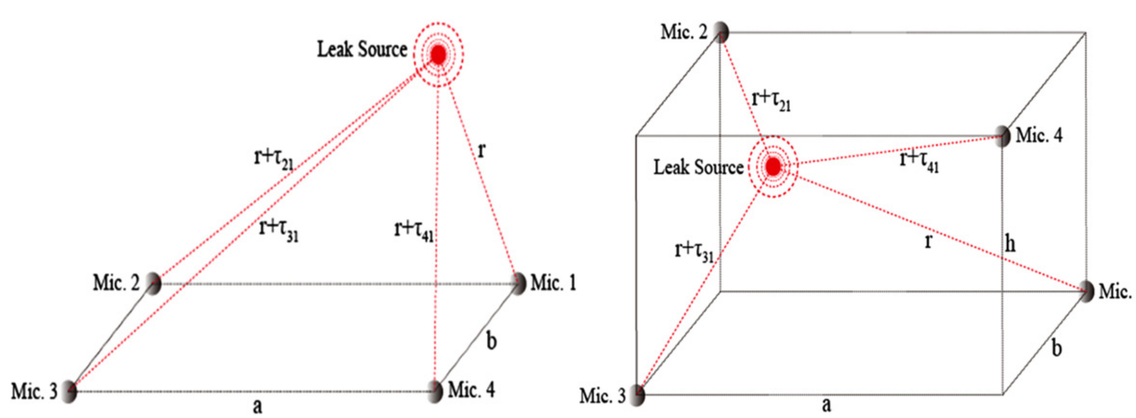

Fig. 2. Four-element array leakage localization geometry.

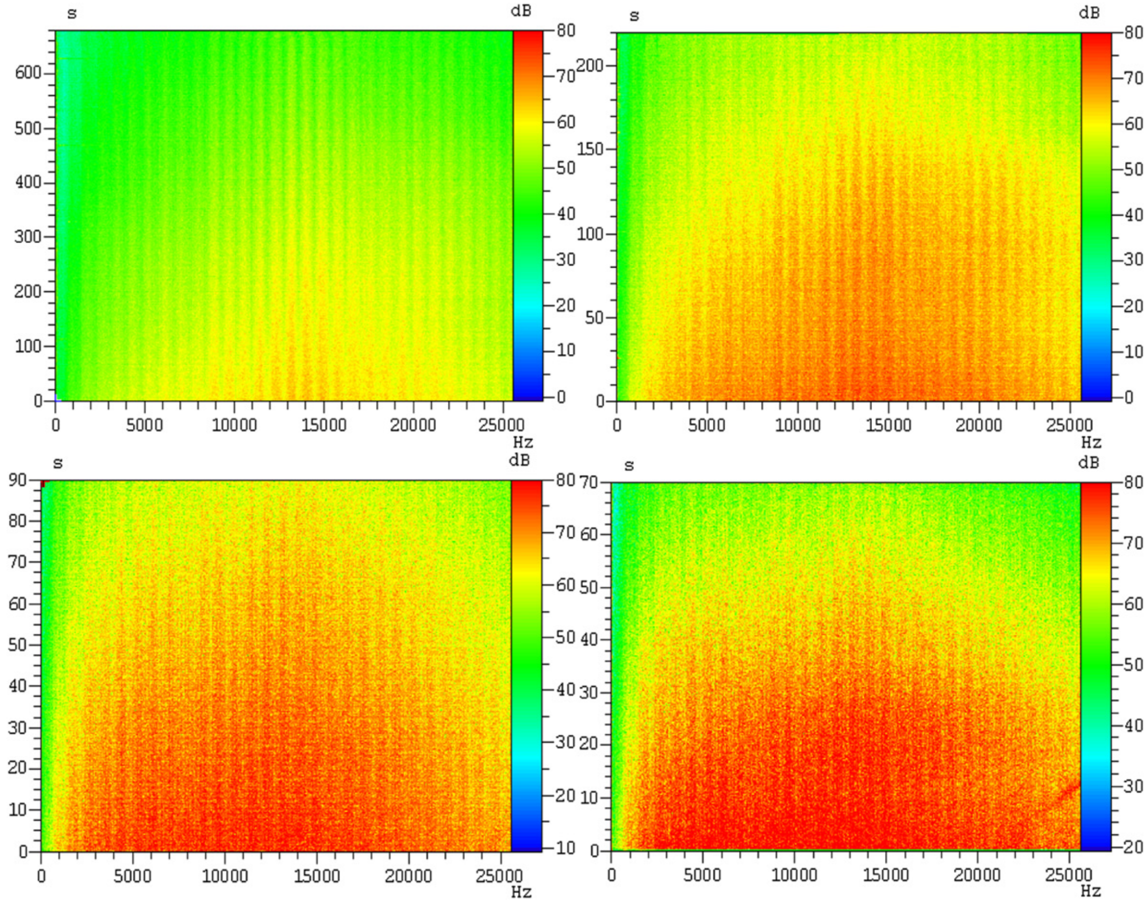

Fig. 3. Time-frequency distribution of leak jet noise from a 1–4 mm aperture.

The results of the time delay estimations are shown in Fig. 7. The graphs show that stable and sharp peaks can be obtained using the ML estimator. The following data are obtained: $\tau_{21} = N_1/F_s = 1.69922$ ms, $\tau_{31} = N_2/F_s = 1.73828$ ms, and $\tau_{41} = N_3/F_s = 3.0957$ ms.

4. Optimization using adaptive Gaussian mutation

The hyperbolic leakage location optimization problem is defined as finding the unique global optimum vector X^*. Vector X^* is associated with the extremum of the hyperbolic location function $F(X) : \Omega \subset R^n \rightarrow R$, which yields $F(X^*) = \min_{x \in \Omega} F(X)$, where Ω is the sensor detection space.

The theory of a standard genetic algorithm (SGA) based on the genetic evolution of species was proposed by John H. Holland in 1975 [18]. SGA is a heuristic searching algorithm based on the mechanics of natural selection and genetics. Its main characteristics are stochasticity, adaptivity, implicit parallelism, and global optimization by probability. However, studies on this theory revealed that it requires large calculations, and has the characteristic of slowly converging as the locally optimal solution becomes near. Premature convergence is indeed often observed in GA literature [19,20].

The procedures applied to optimize the hyperbolic location function optimization as follow:

1) *Decimal floating-point coding*. Traditionally, binary representation has some drawbacks when applied to multidimensional, high-precision numerical problems. Michalewicz posited that floating-point representations outperform binary representations because they are more consistent and precise, as well as can lead to faster execution [21]. Binary representation precision can be enhanced by introducing more bits, which considerably slows down the algorithm. Therefore, in the present study, each chromosome vector was coded as a vector of floating-point numbers. A Gaussian perturbation was then added to ensure that all possible alleles around the best chromosome can be precisely searched. Premature convergence and generating new chromosomes to break off the local minima are hence avoided.
2) *Randomly creating the initial population*. We let the population size N_p be 100. The initial population of parent vectors X_0 was randomly selected from the individual detection range, and we let the initial perturbation vector σ be 0.3. The distribution of initial trials was typically uniform.
3) *Evaluating the fitness value of individuals*. The ith chromosome was assigned with a fitness value according to the fitness function:

$$F_i = \sum_{i=1}^{N_p} f_i(x,y,z)^2 \tag{9}$$

4) *Reproduction*. Each chromosome was assigned a reproduction probability p_i. This probability make it's the chromosome

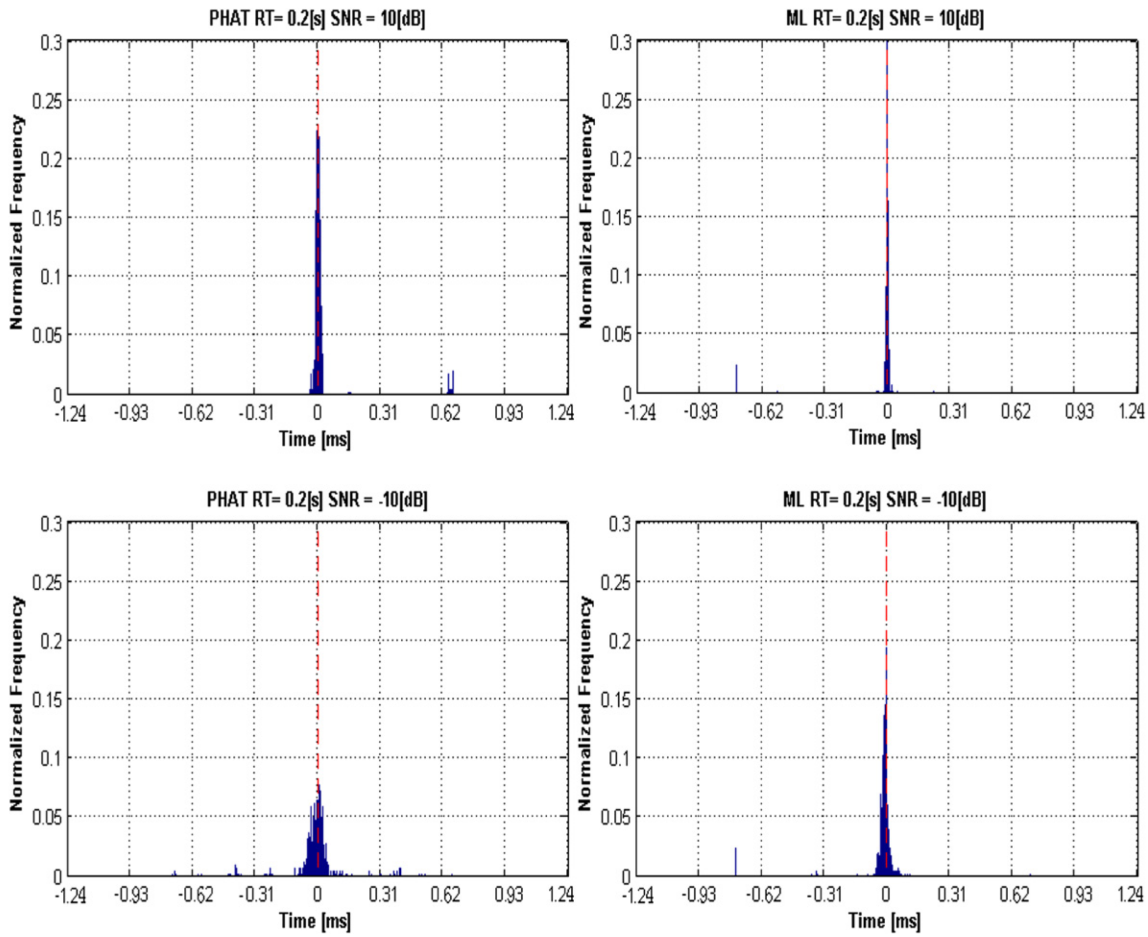

Fig. 4. ML and PHAT estimator histograms at various SNR and RT = 0.2 s conditions.

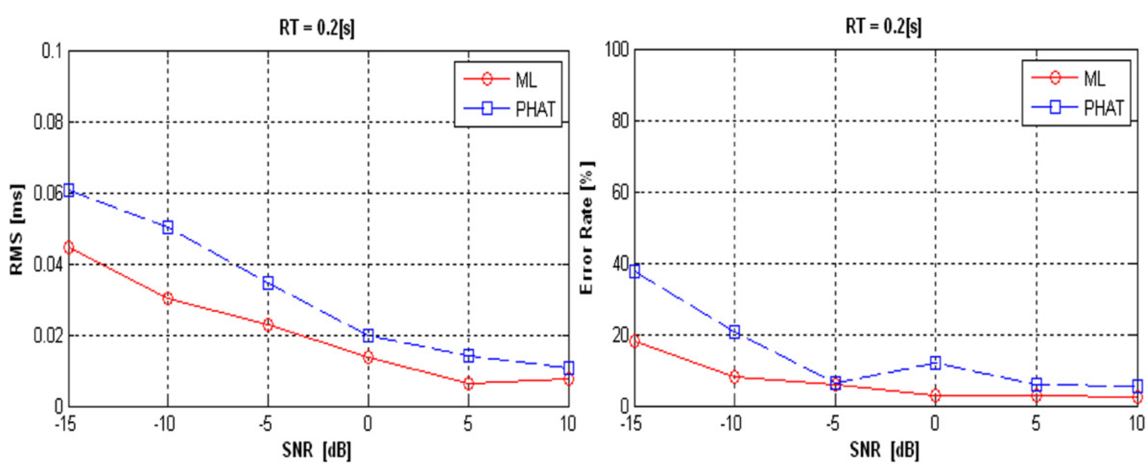

Fig. 5. ML and PHAT estimator error rate and RMSE comparison at various SNR and RT = 0.2 conditions.

selection likelihood proportional to its fitness relative to the other chromosomes in the population. This can be illustrated as:

$$p_r = \frac{F_i}{\sum_{i=1}^{N_p} F_i} \tag{10}$$

5) *Crossover*. According to the assigned probabilities of reproduction p_r, a new chromosome population was generated by probabilistically selecting strings from the current population. With the probability of crossover P_c being 0.8, a crossover operator was applied to two parent chromosomes, resulting in the creation of two offspring chromosomes. This was done by selecting a uniform distribution random position integer j_c [1,2]. The section that appears after the position j_c (in the first string) was spliced with the section appearing before the selected position j_c (in the second string), and vice versa.

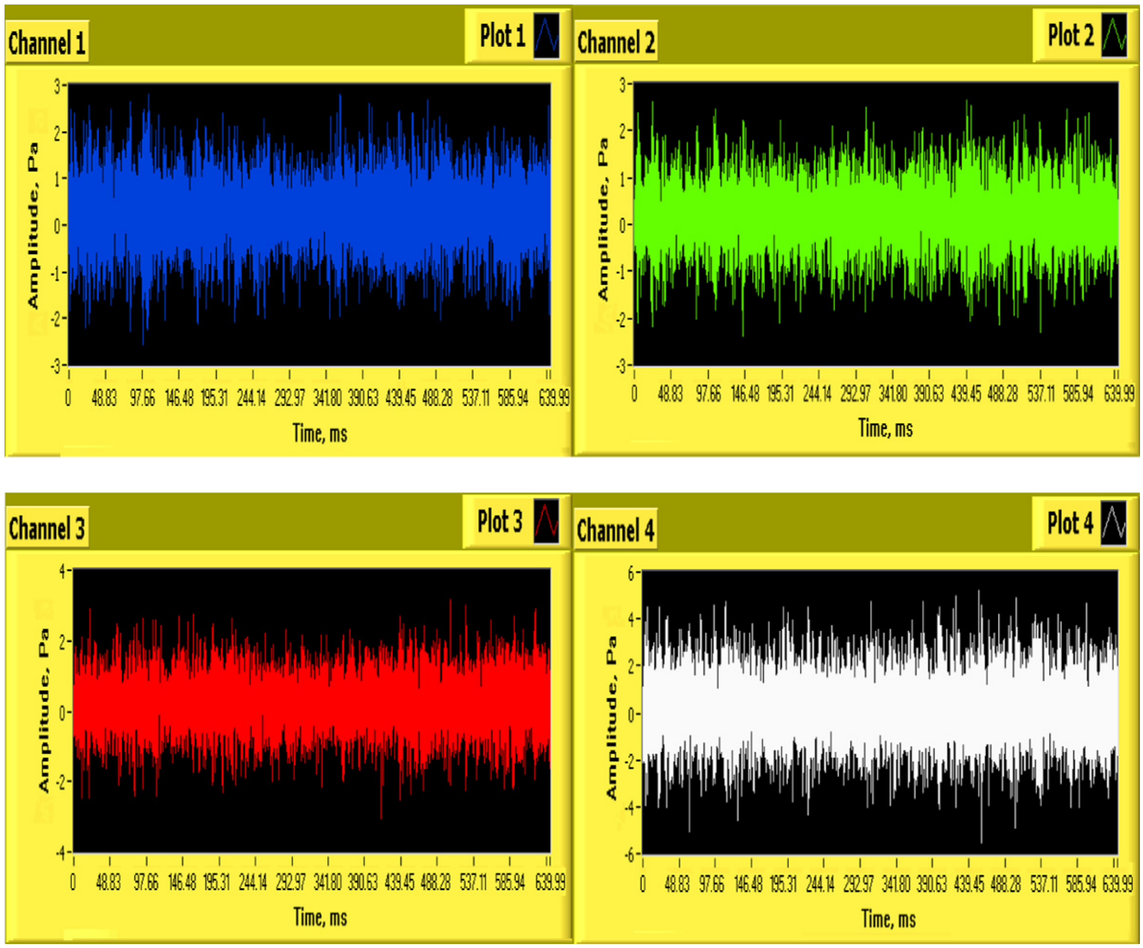

Fig. 6. Time domain waveforms of receivers.

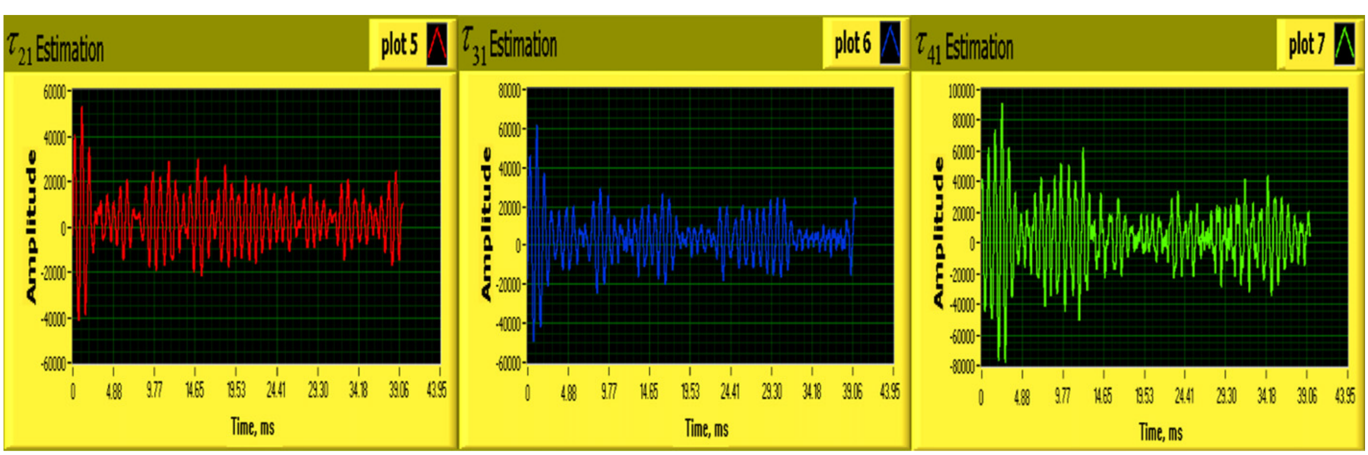

Fig. 7. Time delay ML estimations.

6) *Mutation*. The mutation operator plays a significant role in zooming in on solutions closer to the global optimum, and in zooming out from the local optimum in a heuristic search. The mutation alleles are roughly the same as the genes by a higher probability, and are different by a certain probability. The bit mutation operator universally accepted in the SGA is clearly not suitable for decimal floating-point representations. Therefore, we proposed that each solution vector comprise not only the trial vector X, but also a perturbation vector $\sigma = [\sigma_x, \sigma_y, \sigma_z]^T$, which provides instructions on how to mutate x, and is itself subject to mutation. The mutation was applied to the parent vector, with the probability of mutation $P_{\rm m}$ being 0.3. The offspring solution vector (X', σ') could be described as:

$$\sigma_i' = \sigma_i \exp[\alpha N(0,1) + \beta N_i(0,1)] \tag{11}$$

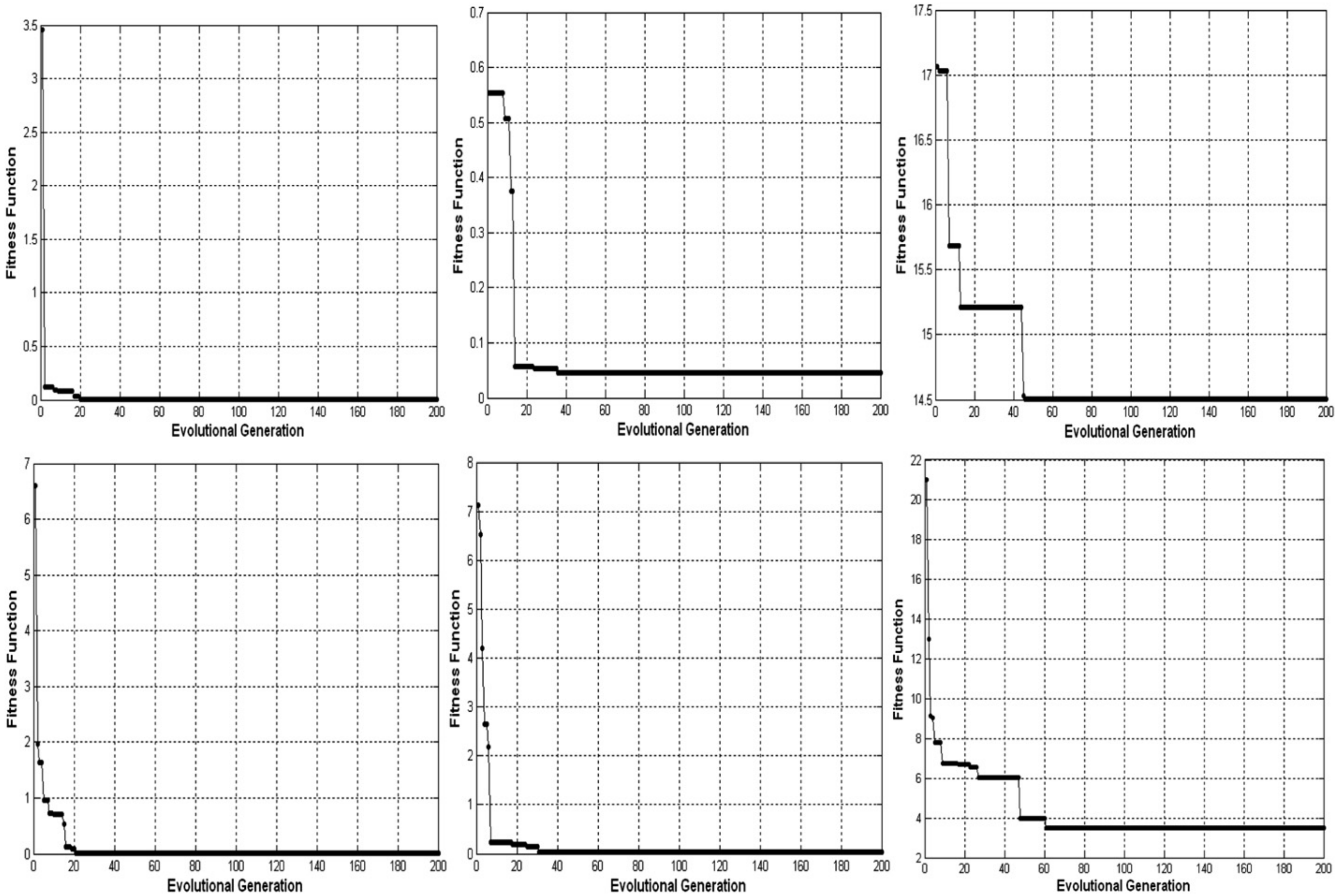

Fig. 8. Evolution curve of the best chromosomes in the population.

$$X_i' = X_i + N(0, \sigma_i') \tag{12}$$

where $N(0, 1)$ represents a single standard Gaussian random variable and $i = 1, 2, \ldots, n$. $N_i(0, 1)$ represents the ith independent and identically distributed standard Gaussian, and α and β refer to the operator set parameters defining the global and individual step sizes, respectively.

7) *Evolution*. The process was halted when a suitable solution was found, or if the available computing time expired. Otherwise, the process proceeded to step (3) above, wherein the new chromosomes were sorted and the cycle was repeated.

5. Effects of time delay estimator errors on the accuracy of the quaternary array localization

For optimizing the plane array localization equations (assuming there is no time delay estimator error), the population needs 22 evolutions, and the optimum fitness value of 0 is robust and accurate. However, when the time delay estimator error is 0.1 ms, the population needs 37 evolutions, and the optimum fitness value is 0.045. When the time delay estimator error is 1 ms, the GA actually performs worse because the population needs 46 evolutions and the optimum fitness value is 14.507.

The stereo array posed a distinct performance advantage over its plane counterpart. Assuming there is no time delay estimator error, the population needs 23 evolutions, and the optimum fitness value is 0. When the time delay estimator error is 0.1 ms, the population needs 31 evolutions and the optimum fitness value is 0.0279. When the time delay estimator error is 1 ms, the GA still performs reliably because it does not suffer from a big bias. The population needs 61 evolutions and the optimum fitness value is 3.4849. The results are illustrated in Fig. 8.

We let there heater tube leakage source coordinates be 5, 3, and 10. As illustrated by τ_{41}, the time delay estimator error varies from -1 to 1 ms, or from -0.1 to 0.1 ms. The GA improved by the adaptive Gaussian mutation operator was used to provide an explicit solution. The coordinate errors of the plane and stereo quaternary array locations are shown in Fig. 9.

As shown in Fig. 9, the coordinate errors are very large in the time delay error varying from -1 to 1 ms, such that the plane array fails to localize the position. In contrast, the range of X, Y, Z error in the stereo array is -0.113–0.358, -0.504–0.789, -0.741–1.22 m, respectively. In -0.1–0.1 ms time delay error scenario, the coordinates are linearized and the error is reduced to 0.79 m in the plane array, whereas the localization error in the stereo array is -0.019–0.021, 0.059–0.061, -0.088–0.092 m.

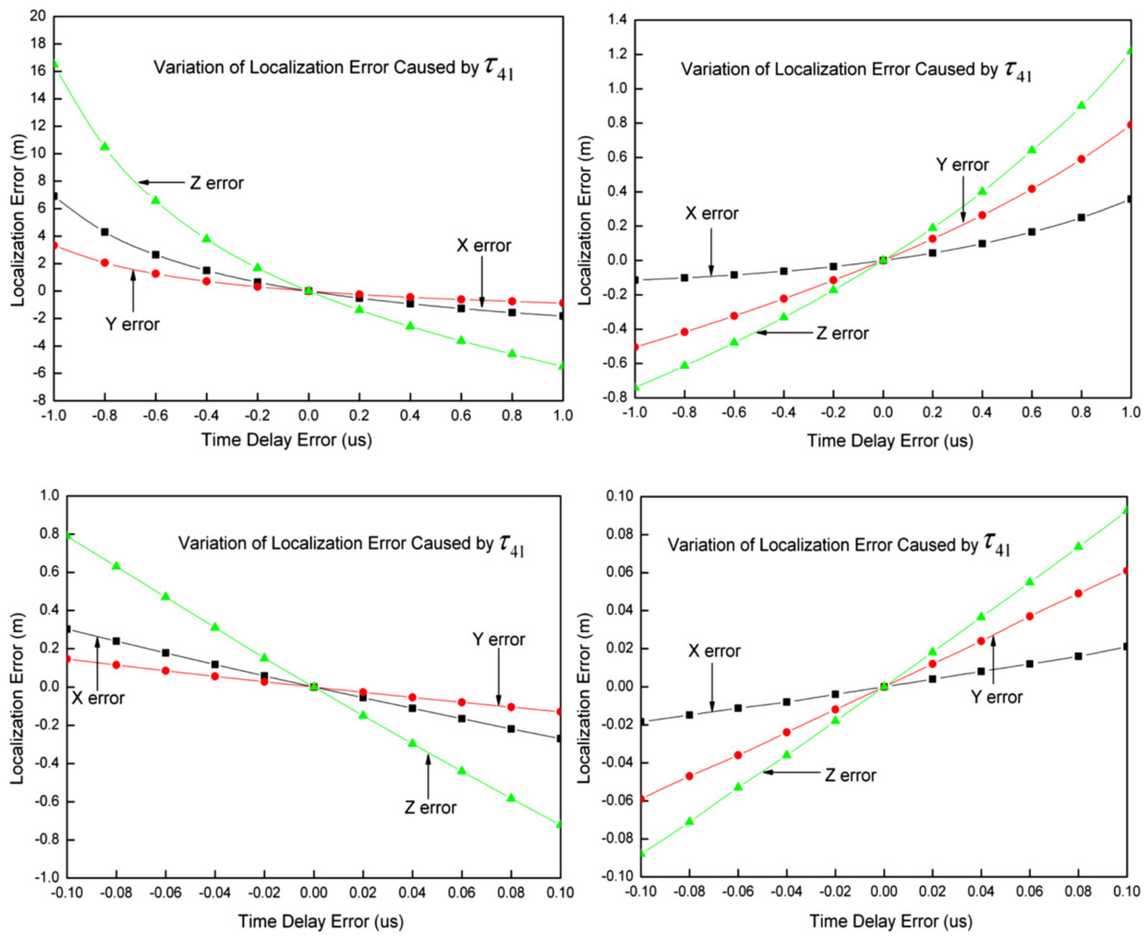

Fig. 9. Comparing the plane to stereo array error curves of the hyperbolic location optimization.

6. Conclusions

Using the quaternary acoustic array for receiving the signal of the boiler tube leakage, the TDOA is obtained using a GCC-based ML estimator. The GA was employed to give an iterative solution based on the set of hyperbolic equations constructed from the TDOA information. The accurate leak position is then located. The following conclusions are derived based on the experiments:

1) The four-element array is suitable for application in a furnace chamber.
2) Based on error rate and RMSE evaluations, the ML estimator is distinctly advantageous over PHAT under noise and favorable reverberation conditions. Stable and sharp peaks can be obtained using the GCC-based ML estimator.
3) The adaptive Gaussian mutation operator used in the GA (encoded as a floating-point) can be used to search for the global optimum parameters by probability calculations. Initial guesses and distant source assumptions are hence avoided.
4) Time delay estimator errors greatly affect the accuracy of localization. The stereo array can fix the leak position in the time delay estimator error permitted range of 0.1 ms, whereas that for the plane array is 0.01 ms. Compared with plane array, the stereo array is more robust and accurate but requires more time to converge.

Acknowledgement

The work described in this paper was supported by a grant from National Natural Science Foundation of China: Researches on Acoustic Passive Recognition and Location with Two Arrays Data Fusion for Explosive Leakage of Power Plant Boiler “Four Tubes” (Project no. 50976034).

The authors thank I.S.P.G, Politecnico di Milano research staff for their valuable discussions, comments and support.

References

[1] Björn Widarsson, Erik Dotzauer, Bayesian network-based early-warning for leakage in recovery boilers, Appl. Thermal Eng. 28 (7) (2008) 754–760. doi:10.1016/j.applthermaleng.2007.06.016.
[2] N. Afgan, P.J. Coelho, M.G. Carvalho, Boiler tube leakage detection expert system, Appl. Thermal Eng. 18 (5) (1998) 317–326. doi:10.1016/S1359-4311(97)00054-9.
[3] G.S. Jiang, L.S. An, Y.D. Lu, Numerical study on the sound wave propagation through a row of heat-exchanger tubes in boilers, Proc. Chin. Soc. for Electrical Eng. 26 (12) (2006) 156–160 doi: CNKI: ISSN:0258-8013.0.2006-12-027.
[4] G.S. Jiang, L.S. An, T. Jing, Numerical study on the sound wave propagation through two rows of heat-exchanger tubes in boilers, Proc. Chin. Soc. for Electrical Eng. 26 (17) (2006) 106–111 doi: CNKI: ISSN: 0258-8013 CN: 11-2107/TM.
[5] G.S. Jiang, L.S. An, G.Q. Shen, Numerical study on the sound wave propagation through many rows of heat-exchanger tubes in boilers, Proc. Chin. Soc. for Electrical Eng. 27 (20) (2007) 81–85 doi: CNKI: SUN:ZGDC.0.2007-20-016.
[6] G.S. Jiang, Acoustic behavior of steam leakage from boiler tubes. Ph.D. thesis, North China Electric Power University, 2006.

[7] M.L. Moran, R.J. Greenfield, D.K. Wilson, Acoustic array tracking performance under moderately complex environmental conditions, Appl. Acoust. 68 (2007) 1241–1262. doi:10.1016/j.apacoust.2006.08.008.
[8] L. Jia, The Research on Acoustic Source localization Based on microphone arrays. Master thesis, Tianjin University, 2008.
[9] S.L. Zhu, An extended KALMAN filtering algorithm based on circular array measurement, Acta Armamentarii 22 (2001) 492–495 doi: CNKI: ISSN:1000-1093.0.2001-04-015.
[10] A.N. Bishop, B. Fidan, K. Dogancay, B.D.O. Anderson, P.N. Pathirana, Exploiting geometry for improved hybrid AOA/TDOA based localization, Signal Process. 88 (2008) 1775–1791. doi:10.1016/j.sigpro.2008.01.015.
[11] Raghu N. Challa, Sanyogita Shamsunder, Passive near-field localization of multiple non-Gaussian sources in 3-D using cumulants, Signal Process. 65 (2009) 39–53. doi:10.1016/S0165-1684(97)00206-5.
[12] G.C. Carter, Time delay estimation for passive sonar signal processing, IEEE Trans. Acoust. Speech Signal Process. 29 (1981) 463–470. doi:10.1109/TASSP.1981.1163560.
[13] J. Liu, Q.M. Cuiand, X.F. Tao, Improved Taylor series location algorithm for cooperation networks, J. China Univ. Posts Telecommun. 14 (2007) 38–44. doi:10.1016/S1005-8885(07)60123-X.
[14] Y.T. Chan, K.C. Ho, A simple and efficient estimator for hyperbolic location, IEEE Trans. Signal Process. 42 (1994) 1905–1915. doi:10.1109/78.301830.
[15] G.Q. Shen, L.S. An, G.S. Jiang, Simulation of time delay estimation in acoustic pyrometry in power plant boiler, Proc. Chin. Soc. Electrical Eng. 27 (11) (2007) 57–61 doi: CNKI: SUN:ZGDC.0.2007-11-010.
[16] J. Allen, D. Berkley, Image method for efficiently simulating small-room acoustics, J. Acoust. Soc. America 65 (1979) 943–950.
[17] M. Brandstein, H. Silverman, A Practical Methodology For Speech Localization With Microphone Arrays Technical Report. Brown University, 1996.
[18] J.H. Holland, Adaptation in Natural and Artificial Systems. University of Michigan Press, Ann Arbor, 1975.
[19] D.B. Fogel, An introduction to simulated evolutionary optimization, IEEE Trans. Neural Netw. 5 (1994) 3–14. doi:10.1109/72.265956.
[20] E. Sidiropoulos, P. Tolikasa, Genetic algorithms and cellular automata in aquifer management, Appl. Math. Model. 32 (4) (2008) 617–640. doi:10.1016/j.apm.2007.01.005.
[21] Z. Michalewicz, Genetic Algorithms + Data Structures = Evolution Programs. Springer-Verlag, New York, 1992.